

Modular Field Robots for Extraterrestrial Exploration

Troy Cordie^{1,2}, Ryan Steindl¹, Ross Dungavell¹, Tirthankar Bandyopadhyay¹

Modular design methodology enables rapid reconfigurability for functional changes, robustness to failures and space utilisation for transportation. In the case of planetary exploration robots, there is promise in modular robots that are able to reconfigure itself for exploration of unknown terrains.

This paper presents a design and controller architecture for modular field robots that can be rapidly assembled in a variety of functional configurations. A key challenge of building a functional robot out of modular units is the ability to seamlessly add, remove and replace individual units to enable functional improvements as well as adapt to terrain requirements. An added benefit of modularity is the ability for graceful degradation through reconfigurability such as detaching a module or adaptation of motion models to actuator failure.

We present a representative modular wheel design and a distributed controller architecture able to create a range of bespoke multi-wheeled configurations capable of traversal on a variety of terrains during simulated failure scenarios. The self-contained wheeled unit has energy, computation communication, and actuation modules and does not require any modification or physical customization in the field during deployment enabling a seamless plug and play behavior. The hierarchical control structure runs a body controller node that decomposes a whole body motion requested from a higher level planner to generate a sequence of actuation goals for each of the modules, while a local controller node running on each of the modules ensures that the desired actuation is adapted to the configuration, load and terrain characteristics.

We present results of the controller adapting to multiple terrains and failure modes with various robot configurations both in a controlled environment as well as in a field deployment scenario.

I. INTRODUCTION

Robotic platforms deployed for extraterrestrial exploration have no capacity for repair or replacement parts. This isolation means that any problem encountered needs to be overcome to keep the mission alive. The Mars rover has faced problems including actuator failure and becoming bogged in the terrain. When the mission has been able to continue a compromised control strategy has been adopted, such as dragging a wheel. Though when strategies to free a platform have been unavailable missions have ended. This paper proposes the use of modular wheels to overcome some of the problems encountered on such missions. The position independent nature of the actuators allows the nominal front of the platform to shift, allowing operations with failed actuators. While modularity enables the platform to

continue operations after suffering a trapped or failed module ejecting the impacted component from the system. The NeWheel system see figure 1 offers a test bed for developing this style of behaviour.

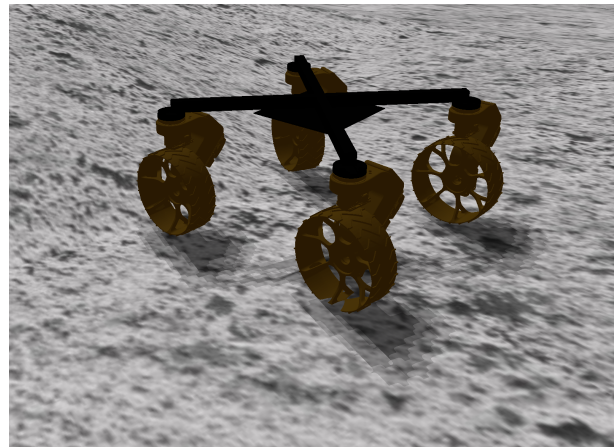


Fig. 1: NeWheel platform depicted in Gazebo simulation Moon analogue

¹ The Robotics and Autonomous Systems Group, CSIRO, Pullenvale, QLD 4069, Australia.

² The Robotics and Autonomous Systems Group, Queensland University of Technology, Brisbane, QLD, 4000, Australia

The work in this project was fully funded by the CSIRO Robotics and Autonomous Systems Group. All correspondence should be addressed to troy.cordie@csiro.au or tirtha.bandy@csiro.au

The remainder of the paper is structured as follows: Section II explores the existing literature of modular robotics and their applicability to extraterrestrial explo-

ration. Our strategy for platform adaptation to failure is laid out in section III. Section IV introduces the modular wheel system used in both simulated and hardware testing conducted for this paper with an overview of the controller and its ability to adapt. Testing was primarily carried out in simulation and is detailed in section V with some of the testing repeated on the platform in section VI, and lastly, section VII summarises the results of this paper.

II. LITERATURE

Since the Russian Lunokhod-1 rover landed on the surface of the moon in 1971 [1] humans, have sent robotic rovers to extraterrestrial bodies to explore and send back data. These rovers cut off from maintenance and repair survive until their sensors and actuators age and decay to a point they are no longer able to operate. Mars rovers Spirit and Opportunity far exceeded their battery life expectancy but at the end of their mission began to reach the limits of their actuators and sensors. In the course of their mission both suffered failures resulting in the need to change control strategies as noted by Townsend [2]. These changes included driving both platforms backwards for large parts of their deployment. For Spirit, this was to reduce the drag of a misaligned wheel and, in the case of Opportunity, to reduce loading on a damaged wheel [3]. Spirit survived with approximately 17% less efficiency until 2009 when it became bogged in soft soil and became a static science platform before finally becoming uncontactable in 2010.

The class of wheeled legged robots shows promise to overcome some of these challenges. In this area, designs vary substantially with each wheeled legged platform proposing different configurations and degrees of limb articulation. Wheeled legged platforms offer the ability to reconfigure platform characteristics such as footprint, ground clearance and body pose. These platforms include All-Terrain Hex-Limbed Extra-Terrestrial Explorer (ATHLETE) [4] and [5], The Mars Analog Multi-Mode Traverse Hybrid (MAMMOTH) [6] and [7], Scarab lunar drilling rover [8] and Wheeled Actively Articulated Vehicle (WAAV) [9] and [10]. Multiple versions of the kinematic for such reconfigurability exist including the work by Alamdari [11], [12] and [13], Sreenivasan [14] as well as the generic models such as [15] by Kelly. By reconfiguring the limb attached to a damaged wheel, the platforms could continue without the misaligned wheel suffered by Spirit. Additionally, the wheeled leg class of platforms has demonstrated the ability to walk out of situations when wheels become bogged or the terrain difficult to pass. This concept has been shown by Klamt [16]. Wheeled legged platforms show promise and have demonstrated capabilities that could have overcome the scenario that trapped Spirit. This

additional reconfigurability comes at the cost of mass, energy usage and complexity. The addition of legs to the platform also adds additional motors sensors and locking mechanisms [17] with each of these adding weight a consideration for transportation to the surface and while deployed as noted by [4]. All of these platforms would, however, suffer the same fate as Spirit should a wheel become stuck - relegated to a static sensing platform.

This paper proposes combining the benefits of reconfigurability with the noted ability of modular robot systems to gracefully degrade [18], [19]. In their simplest form, Murphy [20] describes modular robots as a mother robot with a deployable daughter platform. This style of mother and daughter deployment will be seen on Mars with the planned 2020 Mars helicopter [21]. These platforms have also shown that by reconfiguring, a system can produce platforms with distinctly different capabilities with the same components [22], [23].

At the other end of complexity and component numbers are the modular systems comprised solely of homogenous modules. Systems such as Superbot [24], [25] and SMORES-EP [26], [27] modules illustrate the possibilities of modular, reconfigurable systems. Each of the Superbot and SMORES-EP systems allows multiple platform configurations capable of performing simple tasks. As noted in [26], these systems reach hardware limitations with the example of SMORES-EP capable of supporting 3.1 of its modules when cantilevered restricting the size and the maximum number of components deployed.

Platforms such as Snapbot [28], [29], [30] and Snake Monster [31] connect modular component around a purpose designed torso. Both platforms demonstrate mobility with different numbers of modules attached. This functionality would allow these platforms to abandon failed or faulty modules to maintain system functionality. The torso on both Snapbot and Snake Monster presents a single point of failure. As the torso provides all of the communication and planning for the limbs, its failure would stop any further function. This work looks to incorporate the platform reconfigurability of wheeled legged platforms with the ability to abandon faulty modules from a dumb torso of modular robotics. This combined strategy is laid out in the following section proposing platform adapting until the deployment is risked and ejecting modules if required.

III. STRATEGY FOR ROBUSTNESS

A reconfigurable modular wheeled platform deployment faced with actuator failure could eject the defective wheel and continuing as an n-1-wheeled platform. While this approach is a core strategy for proposed for modular robots deployed in the field, it represents a loss of hardware and would be avoided if possible. Retaining

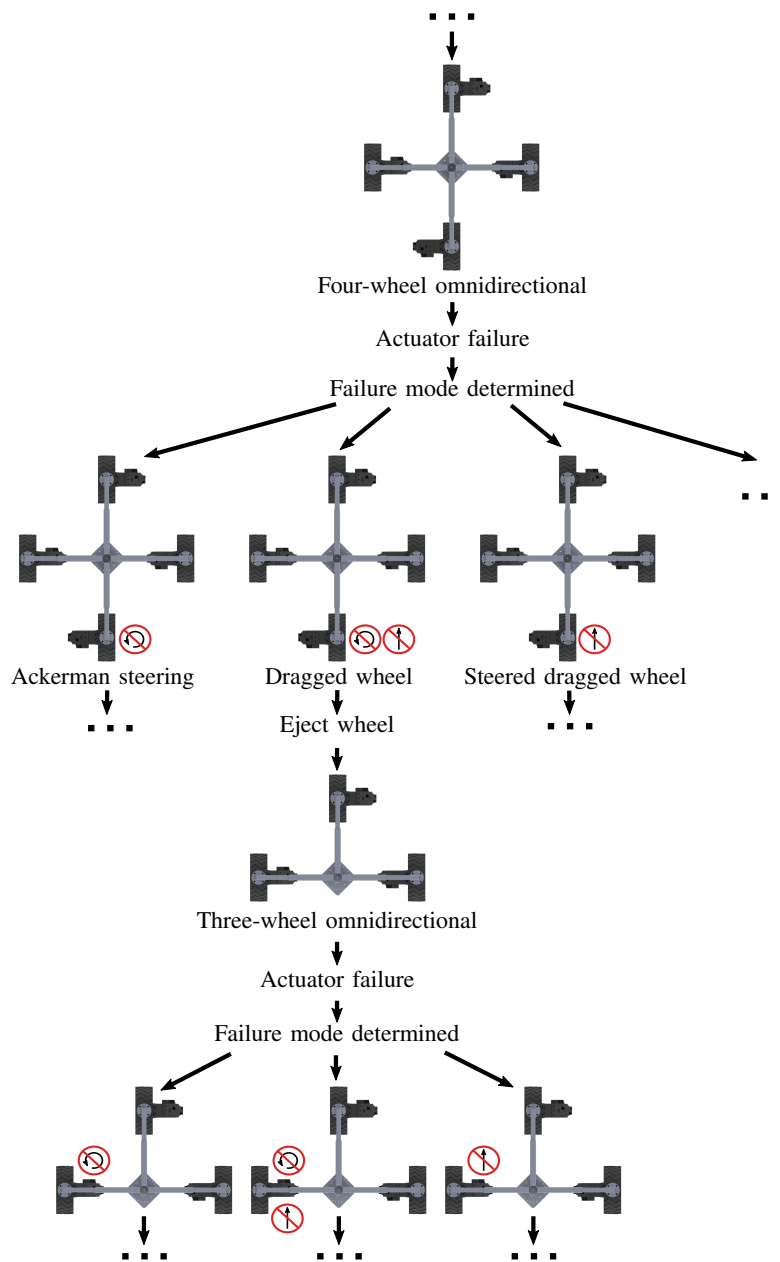


Fig. 2: Partial diagram of a four-wheeled modular robot decaying to the point of ejecting a wheel. Followed by the failure of a module in the three-wheeled platform.

equipment is the priority until it represents a risk to the mission. This work explores strategies to keep defective wheels through some potential failure modes. The potential failure modes are: the failure of the drive motor, failure of the steering motor and the combined failure of the steering and drive motors. In plots and figures depicting the robot's configuration an actuator failure is indicated with either the failed steering or the failed drive icons seen in Figure 3. Figure 2 is a decision tree for the transition from four fully functional wheels to a partially



Fig. 3: Icons indicating failure of an actuator from left to right: failure of a steering actuator, failure of the drive actuator.

functional three-wheeled platform. Failure responses have been explored for the four and three-wheeled systems

as they have the least ability to reconfigure by removing a wheel. These two configurations are reflective of the last remaining components as the system fails or an exploratory platform cut off from replacement parts.

The proposed strategy retains partially damaged or broken wheels through adapting the control strategy based on the hardware available. Read from the top Figure 2 proposes an omnidirectional control strategy for a platform with functional wheels. As failure modes are detected, the appropriate motion mode is adopted. In the case of the failed steering/drive motor, the dragged wheel strategy is proposed. If this wheel becomes a liability, it can be ejected from the system producing a three-wheeled platform capable of omnidirectional motion. The remaining three-wheeled platform has scope to cope with failed actuators.

Edge cases for this proposed strategy are numerous and will not be explored in this work. Situation and platform dependent solutions would be required.

IV. NEWHEEL (ANY WHEEL)

The NeWheel system has been designed to allow fast reconfigurability before or during deployment. This reconfigurability is variable size, shape and module numbers within the system and not dependent on symmetric configurations. These configurations range from large numbers of wheels working collaboratively to individual wheels operating with passive wheels. When combined in large groups the NeWheels could move heavy objects or if combined with rocker bogie links could explore the surface. When a single NeWheel is combined with two passive wheels a tricycle motion model is developed requiring the least power of all the configurations. Previous work carried out with the NeWheel system demonstrated its ability to operate in different configurations and be rapidly redeployed when inspecting dilapidated buildings [32]. The following sections introduce the wheels and controller to demonstrate our proposed strategy possible.

A. Modular Wheels

The NeWheel modules are self-contained, two degrees of freedom powered caster wheels as seen Figure 4. First introduced in [33] each wheel achieves the desired velocity and steering angles with the use of two onboard motors, a battery and onboard computing. In addition to controlling driving and steering velocity, the onboard computer permits inter-wheel communication via WiFi. The location of the power supply and computing on the link between the steering and the driving motors allow the body-wheel connection to rotate continuously. The use of 3D printing has allowed for rapid replacement of parts and design modifications between iterations.

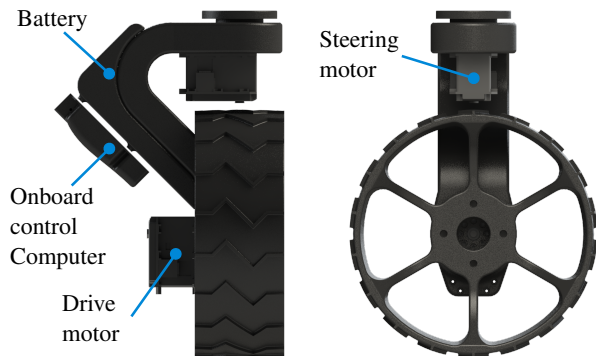


Fig. 4: Current iteration of the NeWheel module

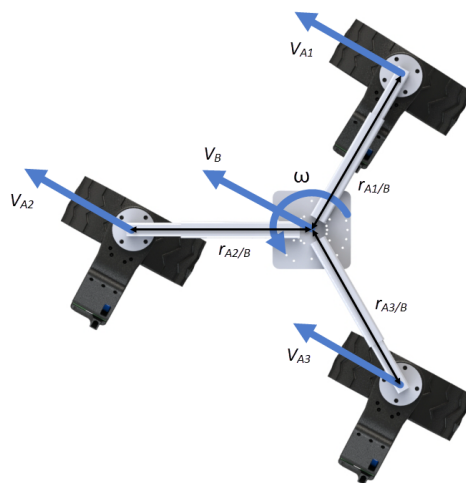


Fig. 5: NeWheel platform configured with the instantaneous centre of rotation at the centre of three wheels. The combined velocity of the three connected wheels produce the desired linear and angular velocity of the body.

B. Controller

The controller designed for the NeWheel system is central to the system's ability to reconfigure quickly and redeploy. It is based around a parametric robot model that once modified propagates through the remainder of the system and generates the controller. The generated controller maintains body velocity by calculating the relative velocity of each wheel see equations 1 and 2. Each wheel independently maintains its own desired velocities and heading, figure 5 shows three NeWheels achieving the desired body linear and angular body velocity.

$$v_w \dot{i} = v_B + \omega_B \times r_{wi/B} \quad (1)$$

$$\alpha_w \dot{i} = \alpha_B + \omega_B^2 \times r_{wi/B} + \omega_B \times (\omega_B \times r_{wi/B}) \quad (2)$$

The implementation of a velocity controller allows movement of the nominal centre of the platform or instantaneous centre of rotation (ICR). Moving the ICR produces different platform behaviour from the same configuration with the same input velocities emulating multiple motion models. Locating the ICR centrally between the wheels attached to the platforms allows Non-holonomic Omnidirectional motion within the body of the platform, as seen in the top left of Figure 6. The top right of Figure 6 show the ICR located on the axis of rotation of the rear wheels, by restricting the control input to $[x, \theta]$ produces a platform with Ackerman steering. Similarly, tricycle steering is produced in platforms with three-wheels see the bottom right of Figure 6. Finally, by configuring IRC between both pairs of wheels sets the platform as differential drive or skid steer see the bottom left of Figure 6.

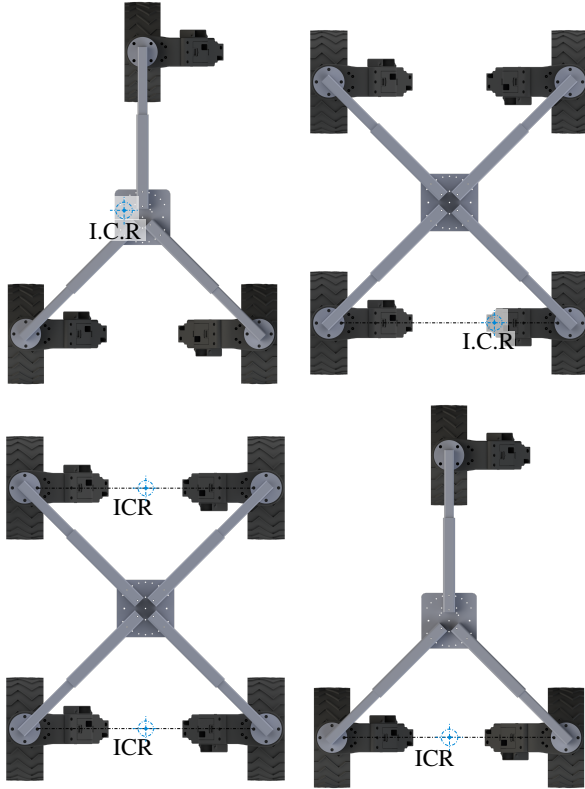


Fig. 6: Clockwise from top left: ICR placed centrally between all attached wheels producing non-holonomic omnidirectional configuration. ICR placed inline with the drive axis of the rear two wheels of a four-wheeled platform confining the platform to Ackerman control. ICR placed inline with the drive axis of the back two wheels of a three-wheeled platform restricting the platform to tricycle control. ICR located between both sets of wheels produces differential drive or skid steer.

$$\zeta_O = \int R(\theta)^{-1} J_1(\beta)^{-1} J_2 \dot{\phi} dt \quad (3)$$

The forward kinematics are derived in equation 3 where $R(\theta)^{-1}$ is the homogeneous transform matrix between the robots pose and the world frame. $J_1(\beta)$ is the $n \times 3$ matrix with each row containing the kinematic constraints of a wheel see equation 4. The pseudo inverse taken to achieve $J_1(\beta)^{-1}$. Where θ_n is the angle from the body to the wheels frame of reference and β_n is the heading of individual wheels.

$$J_1(\beta) = \begin{bmatrix} \sin(\theta_1 + \beta_1) & -\cos(\theta_1 + \beta_1) & -l \cos(\beta_1) \\ \sin(\theta_2 + \beta_2) & -\cos(\theta_2 + \beta_2) & -l \cos(\beta_2) \\ \vdots & \vdots & \vdots \\ \sin(\theta_n + \beta_n) & -\cos(\theta_n + \beta_n) & -l \cos(\beta_n) \end{bmatrix} \quad (4)$$

Under regular operation the steered wheels $J_1(\beta)$ of each wheel is the time-varying function $J_1(\beta_s)$ updating the rotation of the wheels at each time step see equation 5. Wheels with a failed steering actuator have the corresponding $J_1(\beta)$ row $J_1(\beta_f)$ representing a fixed joint as indicated by equation 6.

$$J_1(\beta_s) = \begin{bmatrix} \sin(\theta_{b1} + \beta_{sn}) & -\cos(\theta_{b1} + \beta_{sn}) & -l \cos(\beta_{sn}) \end{bmatrix} \quad (5)$$

$$J_1(\beta_f) = \begin{bmatrix} \sin(\theta_{b1} + \beta_{fn}) & -\cos(\theta_{b1} + \beta_{fn}) & -l \cos(\beta_{fn}) \end{bmatrix} \quad (6)$$

$$J_2 \dot{\phi} = \begin{bmatrix} r_1 & 0 & \dots & 0 \\ 0 & r_2 & \dots & 0 \\ \vdots & \vdots & \ddots & \vdots \\ 0 & 0 & \dots & r_n \end{bmatrix} \begin{bmatrix} \dot{\phi}_1 \\ \dot{\phi}_2 \\ \vdots \\ \dot{\phi}_n \end{bmatrix} \quad (7)$$

Equation 7 is comprised of the $n \times n$ diagonal matrix J_2 of wheel radiuses r_n and the column vector of length $\dot{\phi}$ containing wheel velocities.

For the remainder of the paper, the platform state is described in terms of the actuator input variables β and ϕ . Where β is either the variable β_s for a steerable wheel or β_f for a failed actuator or fixed wheel. The variable ϕ describes the state of the drive motor for each NeWheel, with $\dot{\phi}$ denoting a functioning wheel and $\dot{\phi}_f$ indicating a failed actuator. Individual wheel are noted by the vector $NW_n = [\beta \ \phi]^T$ with a platform (*NeRobot*) defined by a combination of wheel vectors NR . The example below NW_1 as functional while NW_2 has a failed steering actuator, NW_3 a failed drive actuator and

NW_4 represents a failure of both the steering and drive actuators.

$$NR = \begin{bmatrix} \beta_s & \beta_f & \beta_s & \beta_f \\ \dot{\phi} & \dot{\phi} & \dot{\phi} & \dot{\phi} \end{bmatrix} \quad (8)$$

C. Simulations

Experimental results have been captured in the gazebo physics simulator. The simulator uses the parametric Unified Robot Description Format (URDF) model developed for the NeWheel. Allowing fast testing of a variety of different platform configuration. Each simulation starts with the platform pose $\zeta_0 = [0 \ 0 \ 0]^T$ in the units $\zeta = [xm \ ym \ \theta rad]^T$ and a goal set of $\zeta_1 = [5.0 \ 5.0 \ 3.14]^T$. A simple reactive planner guides the platform from the start to the goal position. The start point, goal and level ground terrain were selected to highlight the different platform behaviour available within the same platform configurations by shifting the nominal centre of the platform. This experimental setup limits the variables to the number of wheels attached to the platform and the ICR. Figure 1 shows the four-NeWheeled platform in Gazebo.

V. EXPERIMENTATION

A. Non-holonomic omnidirectional

$$NR = \begin{bmatrix} \beta_s & \beta_s & \beta_s & \beta_s \\ \dot{\phi} & \dot{\phi} & \dot{\phi} & \dot{\phi} \end{bmatrix} \quad (9)$$

or

$$NR = \begin{bmatrix} \beta_s & \beta_s & \beta_s \\ \dot{\phi} & \dot{\phi} & \dot{\phi} \end{bmatrix} \quad (10)$$

An NeWheel platform is capable of non-holonomic omnidirectional motion with any number of functional modules connected. The robot states 9 and 10 show examples of all of the actuators functional for the three and four wheeled configurations. This motion is made possible by the NeWheels drive actuators alignment with the steering actuator allowing the platforms to turn its wheels without moving. For this control strategy, the instantaneous centre of rotation is located centrally between the NeWheels units. This freedom of movement allows manoeuvres such as orientating itself to the goal heading as it approaches the target. An example of this behaviour shown in Figure 7 on a three-wheeled platform. The platform starts with the pose $[0.0, 0.0, 0.0]^T$ and travels to the goal pose of $[5.0, 5.0, 3.14]^T$. The platform achieves this trajectory by rotating its body as it travels along the desired path.

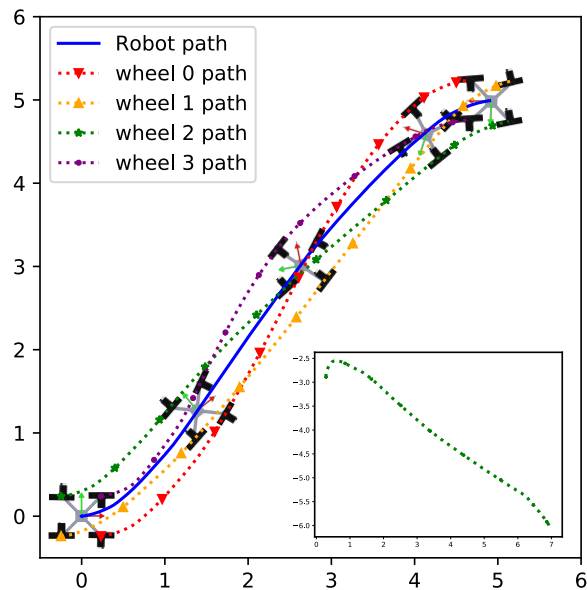


Fig. 7: Four NeWheels moving to the pose $[5.0, 5.0, 3.14]^T [m, m, radian]^T$. The insert depicts the orientation of wheel 2 relative to the platform as it performs the manoeuvre.

B. Ackerman steering

$$NR = \begin{bmatrix} \beta_s & \beta_s & \beta_f & \beta_s \\ \dot{\phi} & \dot{\phi} & \dot{\phi} & \dot{\phi} \end{bmatrix} \quad (11)$$

or

$$NR = \begin{bmatrix} \beta_s & \beta_s & \beta_f \\ \dot{\phi} & \dot{\phi} & \dot{\phi} \end{bmatrix} \quad (12)$$

The failure of a steering actuator as seen in robot configurations 11 and 12 on a robot platform deployed with NeWheels removes a degree of freedom from the platform described previously. This failure prevents the platform from moving perpendicular to the heading of the damaged wheel. An Akerman style motion model is employed to accommodate the loss functionality, minimising the impact on the system. The nominal platform centre is moved to a point along the failed wheels drive axis of rotation to achieve this change in the controller. When the centre is relocated, the symbolic front of the platform passes through the new centre point parallel to the heading of the affected wheel see Figure 8. The remaining NeWheels maintain their full functionality adopting the required heading for driving and steering. Restricting control input for the y-axis(lateral motion) and remapping it as angular velocity results in the platform rotating on the spot to orientate the platform in the desired direction. This functionality, typically not seen in platforms implementing Akerman steering, allows the platform to continue operation in confined spaces.

Figure 9 shows a platform moving to the same final pose $[5.0, 5.0, 3.14]^T$ as figure 7 while using the Ackerman strategy.



Fig. 8: Robot configured to align with the failed steering actuator on the back of a three-wheeled platform

Robot configurations 11 and 12 showing the third NeWheel failing is only indicative. Due to the platforms ability to reconfigure a steering failure is accommodated in any of the wheels by changing the nominal front for the platform. This strategy works for symmetric and non-symmetric platforms alike. In the case of a three-wheeled platform, the resultant platform will operate as either a tricycle with a single steered wheel or with Ackerman style steering and a single fixed wheel.

C. Steered dragged wheel

A steered dead wheel could take many forms and assumptions for this work are as follows. The drive motor is locked in place with no or minimal ability to move, while the steering motor has retained full functionality. The friction model of the wheel/surface follows figure 10 where dragging the wheel perpendicular to the axis of rotation incurs the least friction penalty. Similar to the failed steering actuator in section V-B the location of the failed drive actuator in the robot states 13 and 14 is only indicative due to systems ability to re-orientate.

$$NR = \begin{bmatrix} \beta_s & \beta_s & \beta_s & \beta_s \\ \dot{\phi} & \dot{\phi} & \dot{\phi} & \dot{\phi}_f \end{bmatrix} \quad (13)$$

or

$$NR = \begin{bmatrix} \beta_s & \beta_s & \beta_s \\ \dot{\phi} & \dot{\phi} & \dot{\phi}_f \end{bmatrix} \quad (14)$$

Under the conditions of the single drive motor failure, the platform retains the ability to re-orientate the failed wheel with the direction of travel. When the desired velocity has only a linear component and no angular velocity. The orientation of the platform is modified, locating the dead wheel between the remaining wheels

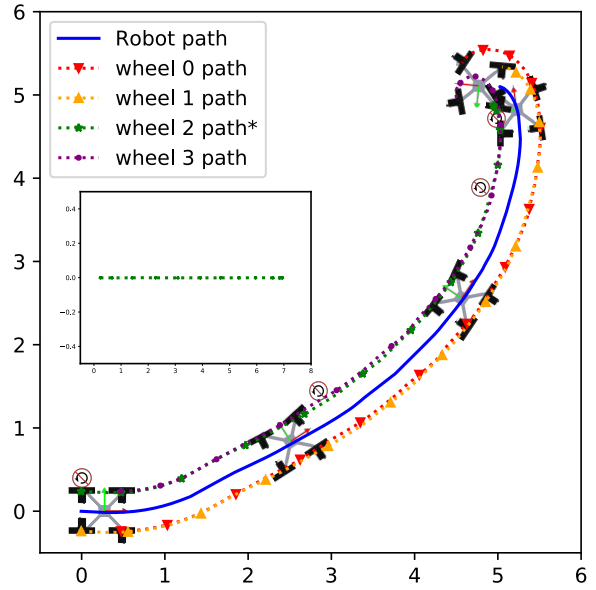


Fig. 9: Four NeWheels moving to the pose $[5.0, 5.0, 3.14]^T [m, m, radian]^T$ using the Ackerman motion model. The insert depicts the orientation of wheel 2 relative to the platform as it performs the manoeuvre.

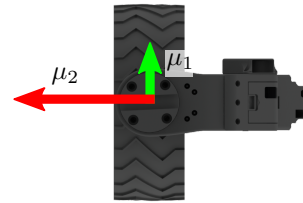


Fig. 10: Assumed friction when dragging dead wheel

as shown in 11a. Allowing the resulting force from the dragged wheel to be distributed between the remaining wheels. Equation 15 is force required to overcome the force induced on the system by the dead wheel where F_f is the force created by the dead wheel dragging and F_{d_i} is the individual force of the functional wheels.

When rotating the platforms ability to shift the ICR allows a platform with a failed drive actuator to shift the ICR outside the body of the robot. Shifting the ICR away from the failed wheel allows management of the torque required of the functional wheels refer to Figure 11b. This system behaviour is captured by equation 16 with the torque on the system generated by the dead wheel $F_f \times r_f$ is counteracted by the torque created by the remaining wheels $F_{d_i} \times r_{d_i}$. Where F_f is the force generated by dragging the dead wheel, r_f is the radius from the ICR to the failed wheel, F_{d_i} is the force generated by individual functional wheels and r_{d_i} is the

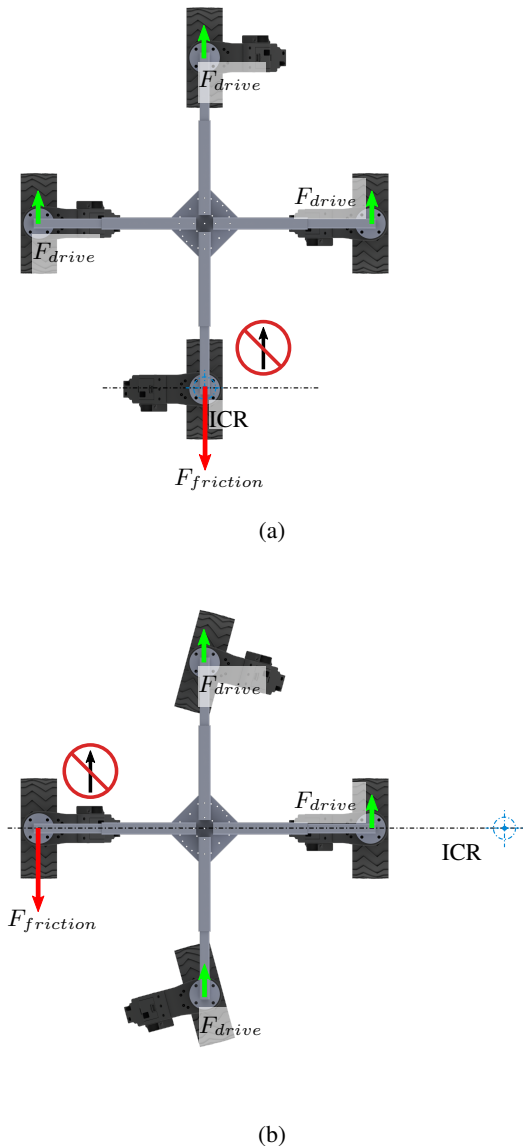


Fig. 11: A four-wheeled configuration with a failed drive actuator (a) shows the platform reorientated to travel without angular velocity and (b) depicts the platform rotating.

radius from the ICR to the individual functional wheels.

$$F_f = \sum_{i=1}^n F_{d_i} \quad (15)$$

$$F_f \times r_f = \sum_{i=1}^n F_{d_i} \times r_{d_i} \quad (16)$$

The two scenarios above assume the remaining wheels can overcome the forces generated by the failed wheel dragging. The remaining wheels must still produce a

functional platform for this strategy to be viable. In the scenario where dragging the failed wheel jeopardises the deployment, the option to eject the wheel must be considered.

D. Dragged wheel

The failure of the drive and steer motors leaves the platform with a dead wheel see robot models 17 and 18. Unlike the steered dragged wheel, the platform must reconfigure using the remaining wheels to minimise the impacts of dragging the dead wheel. This scenario leaves the platform unable to distribute the forces between the remaining wheels evenly. This strategy would be considered before ejecting a wheel from a system few remaining modules.

$$NR = \begin{bmatrix} \beta_s & \beta_s & \beta_s & \beta_f \\ \dot{\phi} & \dot{\phi} & \dot{\phi} & \dot{\phi}_f \end{bmatrix} \quad (17)$$

or

$$NR = \begin{bmatrix} \beta_s & \beta_s & \beta_f \\ \dot{\phi} & \dot{\phi} & \dot{\phi}_f \end{bmatrix} \quad (18)$$

VI. PLATFORM TESTING

Previous testing of the NeWheel platform has demonstrated the system's ability to be rapidly deployed into unstable buildings [32]. This work involved deploying the platform into a decaying building to map and collect data. This work also demonstrated the different capabilities of platform configurations, three-NeWheeled omnidirectional and single NeWheel and two passive wheeled tricycle. This testing showed the tricycles ability to operated on flat terrain and slopes without loose surfaces. Loose ground, and steep slopes proved too much for the tricycle while the three-NeWheeled omnidirectional platform performed minimal slip.

Testing for this paper used a custom built aluminium frame with options for three and four-wheeled configurations. Each wheels configuration within the body can be adjusted radially around the base and the body/wheel links are discretely adjustable in 20 mm increments. This adaptability allows testing of configurations with different sizes, shapes and wheel numbers.

Initially, the platform configured with four functional NeWheels with the ICR placed between them. Commanded to the position $[3.0, 3.0, 3.14]^T$ the system drove to the desired location using the non-holonomic omnidirectional motion model, this was repeated twice more with simulated failure to a steering motor and drive motor. During the failed steering test, the platform drove to the desired pose using an Ackerman control strategy. The final test with the dead drive motor saw the platform struggle to rotate the through 180° for the final pose.

Resetting to the pose to $[0, 0, 0]^T$ the module with the failed drive motor was uncoupled. The platform drove

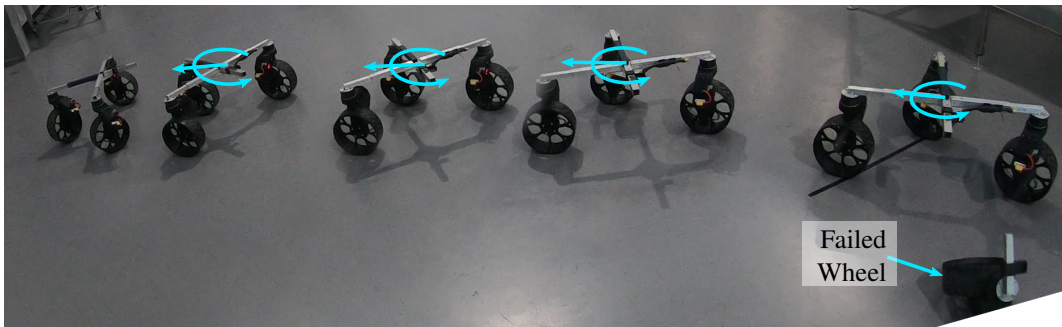


Fig. 12: NeWheel platform testing, the fourth failed wheel is ejected and the three-wheeled continues

away from the fourth wheel achieving the desired pose in a non-holonomic omnidirectional manner see Figure 12

VII. CONCLUSION

This work has proposed a framework for continued operations of reconfigurable modular robots deployed on extraterrestrial bodies. The work noted that wheeled legged platforms enabled some of the proposed functionality at the cost of complexity and mass. Their reconfigurability, combined with wheeled modular robotic units enables the proposed strategy. The strategy laid out proposes modifying the motion model of the deployed platform as actuators decay. Once a module becomes a liability to the mission, modularity allows its removal from the system. The system used to demonstrate this framework was the NeWheel modular robot system; the robot system's hardware and controller having been specifically developed for rapid reconfigurability. The controller's ability to move the instantaneous centre of rotation allows the motion model of the system to change without modifying the hardware. Proposed solutions to steering and drive failures have been tested in both a simulated and simple environment on the robot. The results demonstrated the ability to change the motion model of the platform without needing to modify its configuration. These proposed failures only cover a small number of the possible failures suffered by a deployed platform. Future work includes the automatic adaptation to failure and exploration of further failure modes. In conclusion, reconfigurable modular robots, such as the NeWheel, offer solutions to potential challenges for humanity exploring extraterrestrial bodies.

REFERENCES

- [1] S. Kassel, "Lunokhod-1 Soviet Lunar Surface Vehicle," 1971. [Online]. Available: <https://apps.dtic.mil/docs/citations/AD0733960>
- [2] J. A. Townsend, P. Bellutta, M. Keuneke, M. Seibert, A. Stroupe, J. Wright, E. Ferguson, D. Forgette, J. Herman, H. Justice, and R. Sosland, "Mars Exploration Rovers 2004-2013: Evolving Operational Tactics Driven by Aging Robotic Systems," 2014.
- [3] R. Showstack, "Mars Rover Enters New Phase of Mission," *Eos, Transactions American Geophysical Union*, vol. 91, no. 5, pp. 44–44, 2 2010. [Online]. Available: <http://doi.wiley.com/10.1029/2010EO050003>
- [4] B. H. Wilcox, T. E. Litwin, J. J. Biesiadecki, J. B. Matthews, M. C. Heverly, J. C. Morrison, J. A. Townsend, N. M. Ahmad, A. R. Sirota, and B. K. Cooper, "ATHLETE: A cargo handling and manipulation robot for the moon," *Journal of Field Robotics*, vol. 24, no. 5, pp. 421–434, 5 2007. [Online]. Available: <http://doi.wiley.com/10.1002/rob.20193>
- [5] A. S. Howe, B. Wilcox, M. Barmatz, and G. Voecks, "ATHLETE as a Mobile ISRU and Regolith Construction Platform," 4 2016. [Online]. Available: <https://ntrs.nasa.gov/search.jsp?R=20170007096>
- [6] W. Reid, F. J. Perez-Grau, A. H. Goktogan, and S. Sukkarieh, "Actively articulated suspension for a wheel-on-leg rover operating on a Martian analog surface," in *Proceedings - IEEE International Conference on Robotics and Automation*, vol. 2016-June. IEEE, 5 2016, pp. 5596–5602. [Online]. Available: <http://ieeexplore.ieee.org/document/7487777/>
- [7] W. Reid, A. H. Göktoan, and S. Sukkarieh, "Moving mammoth: Stable motion for a reconfigurable wheel-on-leg rover," in *Australasian Conference on Robotics and Automation, ACRA*, 2014.
- [8] P. W. Bartlett, D. Wettergreen, and W. Whittaker, "Design of the Scarab Rover for Mobility & Drilling in the Lunar Cold Traps," *International Symposium on Artificial Intelligence, Robotics and Automation in Space*, pp. 3–6, 2008. [Online]. Available: <http://repository.cmu.edu/robotics/1104>
- [9] S. V. Sreenivasan, P. K. Dutta, and K. J. Waldron, "The Wheeled Actively Articulated Vehicle (WAAV): An Advanced Off-Road Mobility Concept," in *Advances in Robot Kinematics and Computational Geometry*. Dordrecht: Springer Netherlands, 1994, pp. 141–150. [Online]. Available: http://link.springer.com/10.1007/978-94-015-8348-0_14
- [10] S. V. Sreenivasan and K. J. Waldron, "Displacement Analysis of an Actively Articulated Wheeled Vehicle Configuration With Extensions to Motion Planning on Uneven Terrain," *Journal of Mechanical Design*, vol. 118, no. 2, pp. 312–317, 1996. [Online]. Available: <http://mechanicaldesign.asmedigitalcollection.asme.org/article.aspx?articleid=1444857http://link.aip.org/link/?JMD/118/312/1>
- [11] A. Alamdari and V. N. Krovi, "Design of articulated legwheel subsystem by kinetostatic optimization," *Mechanism and Machine Theory*, vol. 100, pp. 222–234, 6 2016. [Online]. Available: <https://www.sciencedirect.com/science/article/pii/S0094114X16000367>
- [12] A. Alamdari and V. Krovi, "Active Reconfiguration for Performance Enhancement in Articulated Wheeled Vehicles," p. V002T27A004, 2014. [Online]. Available: <http://dx.doi.org/10.1115/DSCC2014-6137>
- [13] A. Alamdari, X. Zhou, and V. N. Krovi, "Kinematic Modeling, Analysis and Control of Highly Reconfigurable Articulated Wheeled Vehicles," in *Volume 6A: 37th Mechanisms and Robotics Conference*. ASME, 8 2013, p. V06AT07A070.

- [Online]. Available: <http://proceedings.asmedigitalcollection.asme.org/proceeding.aspx?doi=10.1115/DETC2013-12401>
- [14] S. V. Sreenivasan and B. H. Wilcox, "Stability and traction control of an actively actuated micro-rover," *Journal of Robotic Systems*, vol. 11, no. 6, pp. 487–502, 1994. [Online]. Available: <http://doi.wiley.com/10.1002/rob.4620110604>
- [15] A. Kelly and N. Seegmiller, "Recursive kinematic propagation for wheeled mobile robots," *The International Journal of Robotics Research*, vol. 34, no. 3, pp. 288–313, 3 2015. [Online]. Available: <http://journals.sagepub.com/doi/10.1177/0278364914551773>
<http://ijr.sagepub.com/cgi/doi/10.1177/0278364914551773>
- [16] T. Klamt and S. Behnke, "Anytime hybrid driving-stepping locomotion planning," in *2017 IEEE/RSJ International Conference on Intelligent Robots and Systems (IROS)*. IEEE, 9 2017, pp. 4444–4451. [Online]. Available: <http://ieeexplore.ieee.org/document/8206310/>
- [17] J. A. T. Machado and M. F. Silva, "An Overview of Legged Robots," *International symposium on mathematical methods in engineering*, 2006. [Online]. Available: https://www.researchgate.net/profile/Manuel_Silva6/publication/258972509_An_Overview_of_Legged_Robots/links/0deec52b1a44f64afb000000.pdf
- [18] M. Yim, W. M. Shen, B. Salemi, D. Rus, M. Moll, H. Lipson, E. Klavins, and G. S. Chirikjian, "Modular self-reconfigurable robot systems [Grand challenges of robotics]," *IEEE Robotics and Automation Magazine*, vol. 14, no. 1, pp. 43–52, 3 2007. [Online]. Available: <http://ieeexplore.ieee.org/document/4141032/>
- [19] S. Murata and H. Kurokawa, "Self-reconfigurable robots," *IEEE Robotics and Automation Magazine*, vol. 14, no. 1, pp. 71–78, 3 2007. [Online]. Available: <http://ieeexplore.ieee.org/document/4141035/>
- [20] R. Murphy, "Marsupial and shape-shifting robots for urban search and rescue," *IEEE Intelligent Systems*, vol. 15, no. 2, pp. 14–19, 3 2000. [Online]. Available: <http://ieeexplore.ieee.org/document/850822/>
- [21] A. Moreno and M. Regina, "Fundamental Study into Rotor Outwash and Dust Kick-up under Mars-like Conditions," 1 2018. [Online]. Available: <https://ntrs.nasa.gov/search.jsp?R=20180008693&hterms=Mars+Helicopter+Mars+Helicopter&q=Nix%3Dmode%2520matchallpartial%7Cmode%2520matchall%26Ntk%3DAI%7CAI%26Ns%3DPublication-Date%7C1%26N%3D0%26No%3D10%26Ntt%3DMars%2520Helicopter%7C%2522Mars%2520Helicopter%2522>
- [22] Z. JIE, T. SHUFENG, and Z. YANHE, "Design and implementation of a modular self-reconfigurable robot," *High technology letters*, vol. 15, no. 3, pp. 227–232, 2009. [Online]. Available: <http://cat.inist.fr/?aModele=afficheN&cpsidt=22146183>
- [23] B. Salemi, M. Moll, and W. M. Shen, "SUPERBOT: A deployable, multi-functional, and modular self-reconfigurable robotic system," in *IEEE International Conference on Intelligent Robots and Systems*. IEEE, 10 2006, pp. 3636–3641. [Online]. Available: <http://ieeexplore.ieee.org/document/4058969/>
- [24] *Autonomous robots*. Kluwer Academic Publishers.
- [25] C.-A. Chen, T. Collins, and W.-M. Shen, "A near-optimal dynamic power sharing scheme for self-reconfigurable modular robots," in *2016 IEEE International Conference on Robotics and Automation (ICRA)*. IEEE, 5 2016, pp. 5183–5188. [Online]. Available: <http://ieeexplore.ieee.org/document/7487724/>
- [26] G. Jing, T. Tosun, M. Yim, and H. Kress-Gazit, "An End-To-End System for Accomplishing Tasks with Modular Robots," *Robotics: Science and Systems XII*, 2016. [Online]. Available: <http://www.roboticsproceedings.org/rss12/p25.pdf>
- [27] J. Davey, N. Kwok, and M. Yim, "Emulating self-reconfigurable robots - design of the SMORES system," in *2012 IEEE/RSJ International Conference on Intelligent Robots and Systems*. IEEE, 10 2012, pp. 4464–4469. [Online]. Available: <http://ieeexplore.ieee.org/document/6385845/>
- [28] J. Kim, A. Alspach, and K. Yamane, "Snapbot : a Reconfigurable Legged Robot," pp. 5861–5867, 2017. [Online]. Available: <https://s3-us-west-1.amazonaws.com/disneyresearch/wp-content/uploads/20170911102717/Snapbot-a-Reconfigurable-Legged-Robot-Paper.pdf>
- [29] S. Ha, J. Kim, and K. Yamane, "Automated Deep Reinforcement Learning Environment for Hardware of a Modular Legged Robot," in *2018 15th International Conference on Ubiquitous Robots (UR)*. IEEE, 6 2018, pp. 348–354. [Online]. Available: <https://ieeexplore.ieee.org/document/8442201/>
- [30] M. Ning, L. Shao, F. Chen, M. Li, C. Zhang, and Q. Zhang, "Modeling and Analysis of a Modular Multilegged Robot with Improved Fault Tolerance and Environmental Adaptability," *Mathematical Problems in Engineering*, vol. 2019, pp. 1–17, 5 2019. [Online]. Available: <https://www.hindawi.com/journals/mpe/2019/8261617/>
- [31] S. Kalouche, D. Rollinson, and H. Choset, "Modularity for maximum mobility and manipulation: Control of a reconfigurable legged robot with series-elastic actuators," in *2015 IEEE International Symposium on Safety, Security, and Rescue Robotics (SSRR)*. IEEE, 10 2015, pp. 1–8. [Online]. Available: <http://ieeexplore.ieee.org/document/7442943/>
- [32] T. P. Cordie, T. Bandyopadhyay, J. Roberts, M. Dunbabin, K. Greenop, R. Dungavell, and R. Steindl, "Modular field robot deployment for inspection of dilapidated buildings," *Journal of Field Robotics*, 2019.
- [33] T. Cordie, T. Bandyopadhyay, J. M. Roberts, R. Steindl, R. Dungavell, and K. Greenop, "Enabling rapid field deployments using modular mobility units," in *Australasian Conference on Robotics and Automation (ACRA) 2016*. Australian Robotic and Automation Association, 2016. [Online]. Available: <https://eprints.qut.edu.au/102223/>